Adv. Geosci., 42, 1–14, 2016
www.adv-geosci.net/42/1/2016/
doi:10.5194/adgeo-42-1-2016

Advances in Geosciences
Open Access
EGU

Precipitation response to El Niño/La Niña events in Southern South America – emphasis in regional drought occurrences

Olga Clorinda Penalba[1,3] **and Juan Antonio Rivera**[2,3]

[1]Departamento de Ciencias de la Atmósfera y los Océanos (DCAO/FCEN), Universidad de Buenos Aires, Buenos Aires, C1428EGA, Argentina
[2]Instituto Argentino de Nivología, Glaciología y Ciencias Ambientales (IANIGLA/CONICET), Mendoza, 5500, Argentina
[3]Instituto Franco-Argentino para el Estudio del Clima y sus Impactos (UMI IFAECI/CNRS), Buenos Aires, C1428EGA, Argentina

Correspondence to: Juan Antonio Rivera (jrivera@mendoza-conicet.gob.ar)

Received: 15 December 2015 – Revised: 11 February 2016 – Accepted: 16 February 2016 – Published: 4 March 2016

Abstract. The ENSO phenomenon is one of the key factors that influence the interannual variability of precipitation over Southern South America. The aim of this study is to identify the regional response of precipitation to El Niño/La Niña events, with emphasis in drought conditions. The standardized precipitation index (SPI) was used to characterize precipitation variabilities through the 1961–2008 period for time scales of 3 (SPI3) and 12 (SPI12) months. A regionalization based on rotated principal component analysis allowed to identify seven coherent regions for each of the time scales considered. In order to identify the regional influence of El Niño and La Niña events on the SPI time series, we calculated the mean SPI values for the El Niño and La Niña years and assessed its significance through bootstrap analysis. We found coherent and significant SPI responses to ENSO phases in most of the seven regions considered, mainly for the SPI12 time series. The precipitation response to La Niña events is characterized with regional deficits, identified with negative values of the SPI during the end of La Niña year and the year after. During El Niño events the precipitation response is reversed and more intense/consistent than in the case of La Niña events. This signal has some regional differences regarding its magnitude and timing, and the quantification of these features, together with the assessment of the SST composites during drought conditions provided critical baseline information for the agricultural and water resources sectors.

1 Introduction

The El Niño-Southern Oscillation (ENSO) phenomenon is the dominant mode of coupled atmosphere-ocean variability on interannual time scales in several regions of the world (Trenberth and Stepaniak, 2001). One of the regions with larger impacts associated with extreme precipitation and ENSO events is Southern South America (SSA). A pioneer study performed by Ropelewski and Halpert (1987) on global scale, based on their previous research for North America (Ropelewski and Halpert, 1986), identified a clear ENSO signal in precipitation patterns over SSA. This signal was characterized with an increase in precipitation over central-east Argentina, Uruguay and Southern Brazil during the summer following the development of El Niño conditions. With focus in South America and surrounding oceans, Aceituno (1988) also showed that the SO-related changes in the large-scale circulation lead to a vast diversity of anomalous regional precipitation regimes. This result was further verified by Grimm et al. (2000), who conducted an analysis of precipitation variability associated with El Niño and La Niña phases through a regional approach. The most important signal usually occurs during the austral summer and autumn after the year of occurrence of El Niño events and during the spring after La Niña years. Penalba et al. (2005) analyzed the probability of exceeding the median during both phases of ENSO, showing coherence between El Niño (La Niña) occurrence and precipitation excess (deficit) over central-eastern Argentina. Nevertheless, this study showed a high degree of regional variabil-

ity in ENSO-related precipitation, which has to be taken into account in precipitation forecasts over large areas.

Impacts of El Niño and La Niña events were evident in the hydrological (Boulanger et al., 2005) and agricultural (Podestá et al., 1999) sectors over SSA and particularly over northeastern Argentina, the southernmost part of Brazil and Uruguay. The precipitation excess associated to El Niño events contribute to the observed excess conditions in soil water content (Spescha et al., 2004) and an increase in about 10 % in soil water storage (Penalba et al., 2014a). River overflows and floods were related with above-normal precipitation linked to El Niño years were extensively documented, particularly over La Plata Basin and its main water courses (Camilloni and Barros, 2003; Chamorro, 2006; Antico et al., 2015). Regarding the trends in precipitation, Barros et al. (2008) demonstrated that half of the annual trends over northeastern Argentina, southern Brazil and Paraguay were associated to the El Niño phase. Even when there is an evidence of the existence of a core region regarding the signal of ENSO in precipitation patterns, other areas of SSA showed a modulation in hydroclimatic variables associated with El Niño and La Niña events. For instance, streamflow excess over the central Andes of Argentina was mainly related to El Niño conditions, while streamflow deficiencies correspond mostly to La Niña occurrences (Compagnucci and Vargas, 1998; Prieto et al., 1999; Rivera et al., 2015). Minetti et al. (2003) showed that La Niña events of 1988–89 and 1995–96 changed the increasing trend slope in annual precipitation over northwest Argentina. In central Argentina, Pasquini et al. (2006) showed that only 3 out of 12 rivers exhibit an ENSO signal, indicating that is not possible to connect the discharge anomalies in the Pampas ranges with the events in the tropical Pacific. The signal of ENSO was observed also in the precipitation records over the Patagonia region (Paruelo et al., 1998; Russián et al., 2010), in combination with a signal from the Southern Annular Mode (SAM) (Silvestri and Vera, 2003; González and Vera, 2010).

This large number of regional studies used different precipitation databases and periods of record, and compared observations from different climatic regions. Moreover, the significance of the ENSO signal in the precipitation records was not often tested, and its length and intensity is also regionally dependent. Based on these considerations, this paper aims to advance in the understanding of the temporal variability of precipitation over SSA at a regional level, with emphasis on the response of precipitation to El Niño/La Niña occurrences. The standardized precipitation index (SPI) is used to characterize precipitation fluctuations over the study area, given that it allows to compare precipitation records from locations with different climate conditions (Moreira et al., 2008). Moreover, the SPI can be calculated for a variety of time scales (Hayes et al., 1999), allowing the quantification of short- and long-term precipitation shortages and excess. Emphasis will be given to the assessment of drought conditions, which are especially important in regions where economic activities are highly dependent on water resources, and particularly affect nations heavily reliant on agriculture, including both subsistence and highly intensive and high technology agricultural practices, as the case of SSA. In this sense, Vicente-Serrano et al. (2011) showed that during La Niña events there is an increase in the probability of drought occurrences in several regions of SSA. Droughts by nature are a regional phenomenon and commonly cover large areas during long periods of time; therefore, it is important to study these events in a regional context (Hisdal and Tallaksen, 2003). These results together with the analysis of SST composites will provide reference information for different sectors related to agriculture and water resources, which can enhance the understanding of seasonal precipitation forecasts.

2 Data

2.1 Precipitation data

The database for the study consists of 56 high-quality monthly precipitation time series that cover the period 1961–2008, obtained through the CLARIS LPB database (Penalba et al., 2014b). These stations are located in the portion of South America south of 20° S, have less than 2 % of missing data and were subjected to quality control procedures, as described in Penalba et al. (2014b). Additionally, a homogeneity control using the Standard Normal Homogeneity Test (Alexandersson, 1986) allowed to identify inhomogeneities in 4 of the 56 precipitation time series, which correspond to climatic jumps and not to instrumental factors. Gap-filling routines were applied through linear regressions with reference time series.

These high-quality time series were used to calculate the SPI, developed by McKee et al. (1993) for drought definition and monitoring. This index quantifies the number of standard deviations that accumulated precipitation in a given time scale deviates from the average value of a location in a particular period. The SPI is a powerful, flexible index that is simple to calculate, it has been recommended by the Lincoln Declaration on Drought Indices (Hayes et al., 2011) and according to Penalba and Rivera (2015) is the most adequate meteorological drought index for SSA. For the calculation of the SPI, the accumulated precipitation time series were divided in 12 monthly series of 48 years, each of them were fitted to a two-parameter gamma probability density function. This distribution appropriately fits the accumulated precipitation in the study region for time scales between 1 and 12 months, which was verified through the Anderson-Darling goodness-of-fit test (Anderson and Darling, 1952) for a confidence level of 95 % (Penalba and Rivera 2012, 2016; Penalba et al., 2016). The 12 probability density functions for each time scale and period were translated to 12 cumulative density functions. Given that the gamma distribution is undefined for $x = 0$, the relative frequency of precipitation

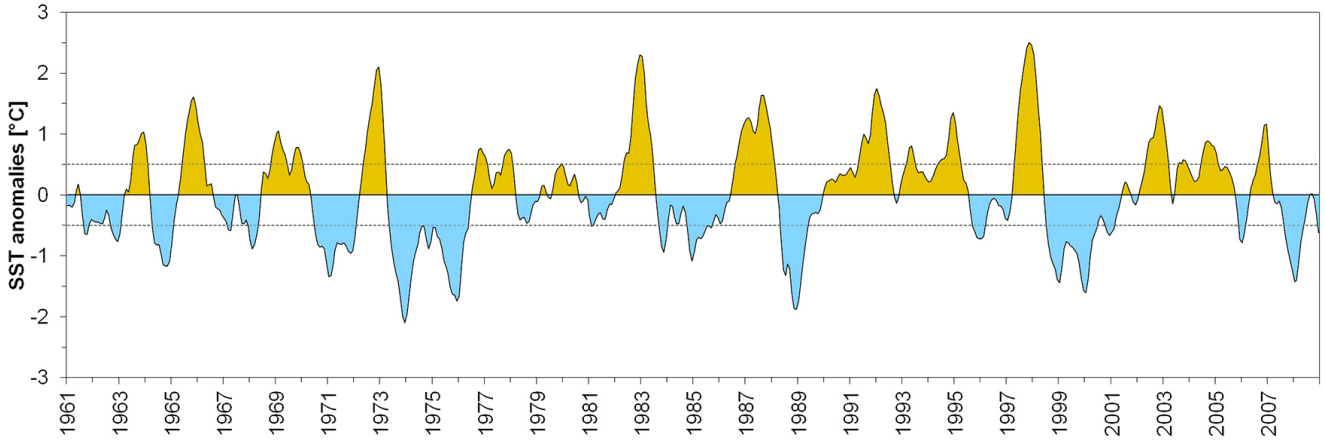

Figure 1. Time series of the Oceanic Niño Index for the period 1961–2008. Dotted lines indicate the ±0.5 °C thresholds.

containing zero values (q) was considered for the cumulative density function:

$$H(x) = q + (1-q)G(x), \quad (1)$$

where $G(x)$ is the gamma cumulative density function. The value of q decreases as the time scale for the accumulation of precipitation increases, being zero for time scales longer than 7-months. This value also shows a seasonal variation; for example, in the case of 3-month accumulation, the higher values of q are observed during the dry season – winter of the southern hemisphere – in semi-arid regions, with a maximum value of 0.1. Finally, an equi-probability transformation from the cumulative density functions to the standard normal distribution with the mean of 0 and the variance of 1 were performed to obtain the SPI.

A detailed description of the calculation of the SPI can be found in Lloyd-Hughes and Saunders (2002). Given that droughts will impact different sectors and activities depending on the time scale over which precipitation deficits accumulate (Edwards and McKee, 1997), in this work, the SPI was computed on time scales of 3 (SPI3) and 12 months (SPI12), representing short-term and long-term droughts, respectively. Short-term droughts used to affect the agricultural sector, while long-term droughts have impacts on the water resources (Guttman, 1999). Both sectors are extremely important in SSA.

2.2 ENSO index

Several indicators have been developed for the definition and monitoring of ENSO conditions, such as the Southern Oscillation Index (SOI, Trenberth, 1984), the Multivariate ENSO Index (MEI, Wolter and Timlin, 1993) and the Trans-Niño Index (Trenberth and Stepaniak, 2001). In this work, the Oceanic Niño Index (ONI), developed by the Climate Prediction Center (CPC) from the National Oceanic and Atmospheric Administration (NOAA), was used to define El Niño/La Niña conditions. The ONI was obtained from the Extended Reconstructed SST v3b (Smith et al., 2008) as a 3-month moving average applied to the SST anomalies over El Niño 3.4 region, located in 5° N–5° S, 120–170° W. A detail of the areas chosen to monitor el SST anomalies related to ENSO can be found in Penland et al. (2010). SST anomalies were calculated based on the 1971–2000 baseline period. El Niño and La Niña events can be defined as 5 consecutive overlapping 3-month period at or above the +0.5 °C anomaly for warm (El Niño) events and at or below the −0.5 °C anomaly for cold (La Niña) events. Finally, El Niño years between 1961 and 2008 are 1963, 1965, 1968, 1972, 1976, 1982, 1986, 1991, 1994, 1997, 2002, 2004, 2006; and La Niña years are 1962, 1964, 1967, 1970, 1973, 1984, 1988, 1995, 1998, 2000 and 2007. It should be noted that the El Niño and La Niña years remain the same if we consider other indices like El Niño 3.4 or the SOI, and minor differences can be observed on a monthly basis, due to the different definition of each index. Nevertheless, changing the baseline period for the calculation of the SST anomalies can introduce some differences in the definition of ENSO years (not shown). Figure 1 shows the temporal evolution of the ONI during the period 1961–2008.

3 Methodology

Using a regional average provides a time series that is a better representation of large-scale processes, and it is easier to deal with one index series (Schonher and Nicholson, 1989). Moreover, it gives a more accurate estimation of the probabilities of observed precipitation (Guttman, 1999). In order to obtain the regional features of precipitation time series, we used the Rotated Principal Components Analysis (RPCA) (Richman, 1986). This methodology was applied in S-mode, which allows to obtain a spatial regionalization and temporal patterns of precipitation in the studied domain. Varimax rotation (Kaiser, 1958) was applied to obtain consistent spa-

tial patterns, retaining the orthogonality and enhancing the interpretability of the results. The variables to be substituted by the principal components derived from the RPCA are the 56 meteorological stations, represented by their SPIs. The scree test of Cattell (1966) was adopted to decide how many PCs to retain in order to separate signal to noise. The maximum loading approach, in which each station is assigned to the component upon which it loads most highly (Comrie and Glenn, 1998), was used to delineate the regions. For both time scales of 3 and 12 months, seven homogeneous regions were obtained, which are climatically and geographically consistent.

Once the SPI homogeneous regions were obtained, the seven regional SPI time series for each of the time scales considered were used to calculate the composites during El Niño and La Niña years (year 0) and the years before (−) and after (+) the events, in line with the methodology proposed by Ropelewski and Halpert (1987). Thus, the analysis of the aggregate composites covers a period of 36 months. SPI average values for each region for the 13 El Niño and 11 La Niña events during the 1961–2008 were calculated, for each of the 36 months centered in the year of beginning of the event, for both SPI3 and SPI12 time series. Since the SPI is standardized, the anomalies can simply be obtained from an average of the values in the years considered. The use of regional composites will allow to identify the El Niño/La Niña signal in a better way than using individual locations, which may only detect anomalies related to a local phenomenon (Chiew et al., 1998). As an example, Fig. 2 shows the composite of SST anomalies over the El Niño 3.4 region during El Niño and La Niña events for the 36 months considered for the analysis of the signal in precipitation. An approximately symmetric behavior between the composites of El Niño and La Niña years is observed, as previously shown by Vicente-Serrano et al. (2005). The largest SST anomalies occur during the summer following the start of the event, typically during the months of November (0), December (0) and January (+) (Fig. 2). For the southern hemisphere seasons, the onset of the El Niño/La Niña events occurs in late autumn or during the beginning of winter and lasts until autumn of the following year. It is expected a precipitation response during these months, although when precipitation is accumulated over several months the response can be delayed. The inter-quartile interval shows that there is a larger dispersion in the composite of the SST anomalies once El Niño event has finished and before the beginning of La Niña conditions. It is expected that this uncertainty also affects the precipitation responses at a regional level.

In order to identify significant changes in the 36 monthly anomalies, we used a bootstrap resampling procedure (Efron and Tibshirani, 1993). The bootstrap is a computing-intensive statistical method that provides a confidence band around the SPI composites. Its advantage is that it is less restricted by parametric assumptions than more traditional approaches (Mudelsee, 2011). The confidence intervals were

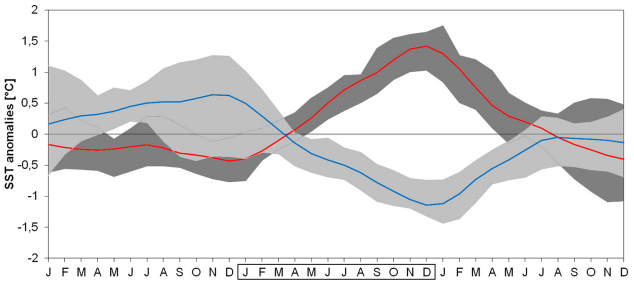

Figure 2. Composite of monthly SST anomalies for El Niño (red line) and La Niña (blue line) during the 1961–2008 period. The 36 month composite starts at January (−) and continues until December (+). Dark (light) grey bands around the composite anomalies represent the inter-quartile interval for El Niño (La Niña).

based on 1000 resamples for the 95 % significance level; therefore, they are given by the interval between the 50th and the 95th largest values. By comparing the values of the monthly SPI composites with the percentile-based confidence interval constructed with the resampling of the SPI values, we can assess if the composites show a significant El Niño/La Niña signal.

4 Results

4.1 El Niño and La Niña signal in precipitation over SSA: SPI3

The regionalization of the 56 SPI3 time series resulted in a total of seven homogeneous regions: CES (Central-East South); P + PN (Pampas and Northern Patagonia); CW (Central-West); CEN (Central-East North); NE (Northeast); SP (Southern Patagonia) and NW (North-West) (Fig. 3). The regional SPI3 patterns account for different temporal variations in precipitation and were ordered taking into account the explained variance of each mode. Positive (negative) values account for above (below) average precipitation periods, and its intensity is proportional to its value, either positive for the excess or negative for deficits. The existence of relatively dry periods which are common in several of the regions is evident, although high frequency variations present in the time series are relevant. Drought events during 1960s and the beginning of 1970s stand out, as the events of late 1980s and mid-1990s (Fig. 3). The spatial extension of these drought events was assessed by Rivera and Penalba (2014), typically covering more than 60 % of the study area.

Figure 4 shows the SPI3 composites during a 36-month period centered in El Niño (left panel) and La Niña (right panel) years for the seven homogeneous regions. It is observed that the months where the influence of El Niño events in the precipitation is significant (marked with red) has considerable regional variations, nevertheless, in all the regions the SPI significant composites are positive (Fig. 4, left panel). For

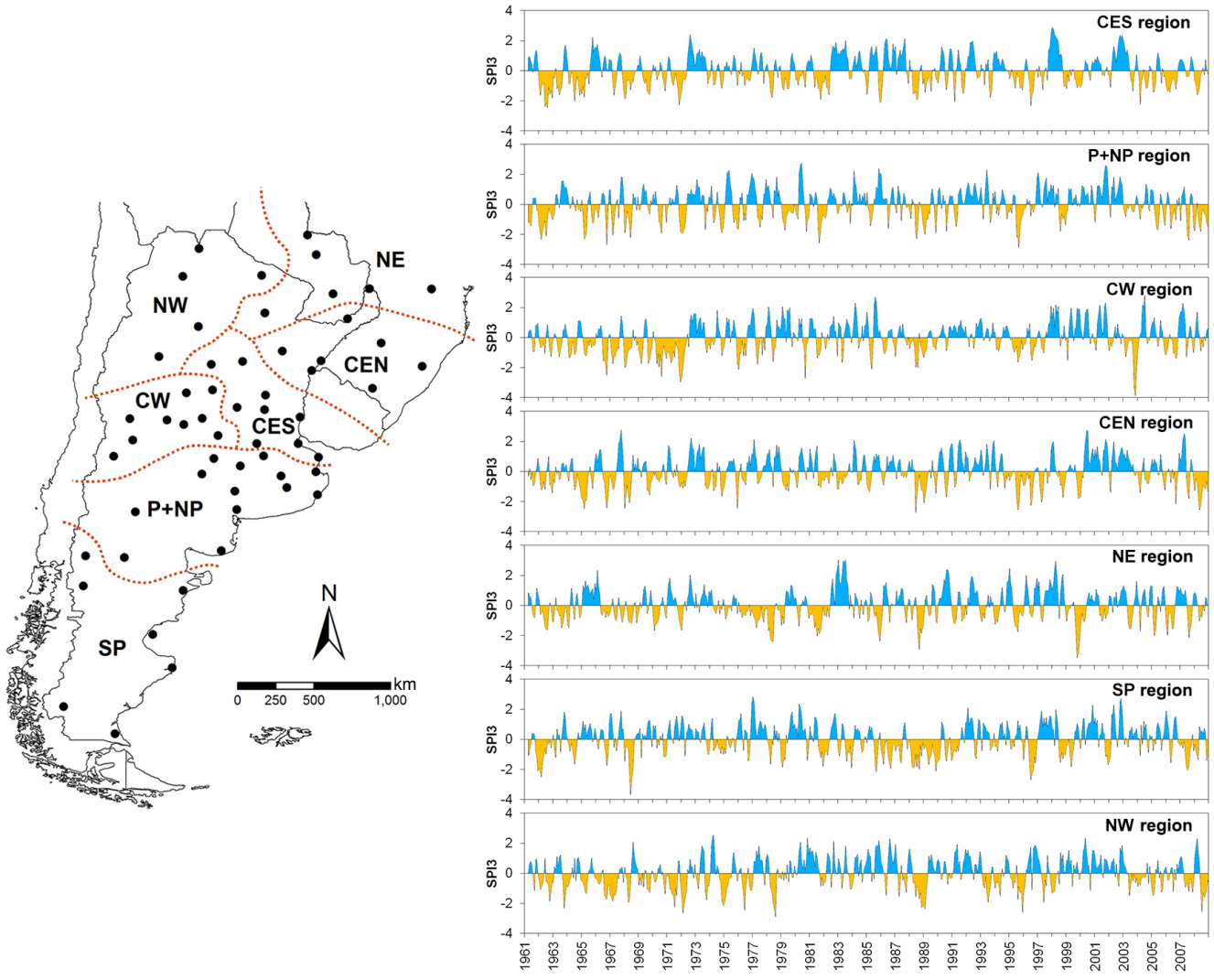

Figure 3. Regions obtained through RPCA applied to the SPI3 time series (left) and its corresponding regional temporal patterns (right).

the CES region, the El Niño influence is significant between December (0) to May (+), although there is a significant positive anomaly during August (0). In the P + NP region the El Niño signal is observed from the month of August (0) to April (+), in line with the average temporal behavior of SST anomalies shown in Fig. 2. The SPI3 in the CW region shows significant anomalies during the period August (0)–February (+). The most consistent response is observed in the CEN region, with significant SPI3 anomalies between October (0) to August (+). The amplitude of the anomalies is close to one standard deviation during the summer months of the year following El Niño development, i.e., when the magnitude of the SST anomalies during El Niño years have the higher values (see Fig. 2).

In the NE region, the El Niño events have a significant influence in precipitation during the period between November (0) and June (+), in line with the signal observed in the adjacent CEN region but with less intensity. In the case of the SP, the response is observed during the months of September (0) to January (+), while for the NW region the El Niño signal is observed between August (0) and December (0). In general, a greater influence of El Niño in the precipitation anomalies were observed in the SPI3 composites of the CEN, NE and CES regions, both in magnitude and duration. Moreover, the temporal evolution of the significant SPI3 composites in these regions is similar to the pattern of the SST anomalies over the tropical Pacific (Fig. 2). It is noteworthy that in the regions of the central portion of SSA during the year preceding El Niño development there is a tendency to have precipitation deficits, something previously identified by Grimm et al. (2000).

The right panel of Fig. 4 shows the regional SPI3 composites during the 36-month period centered in La Niña years. In most of the regions the influence of La Niña events in pre-

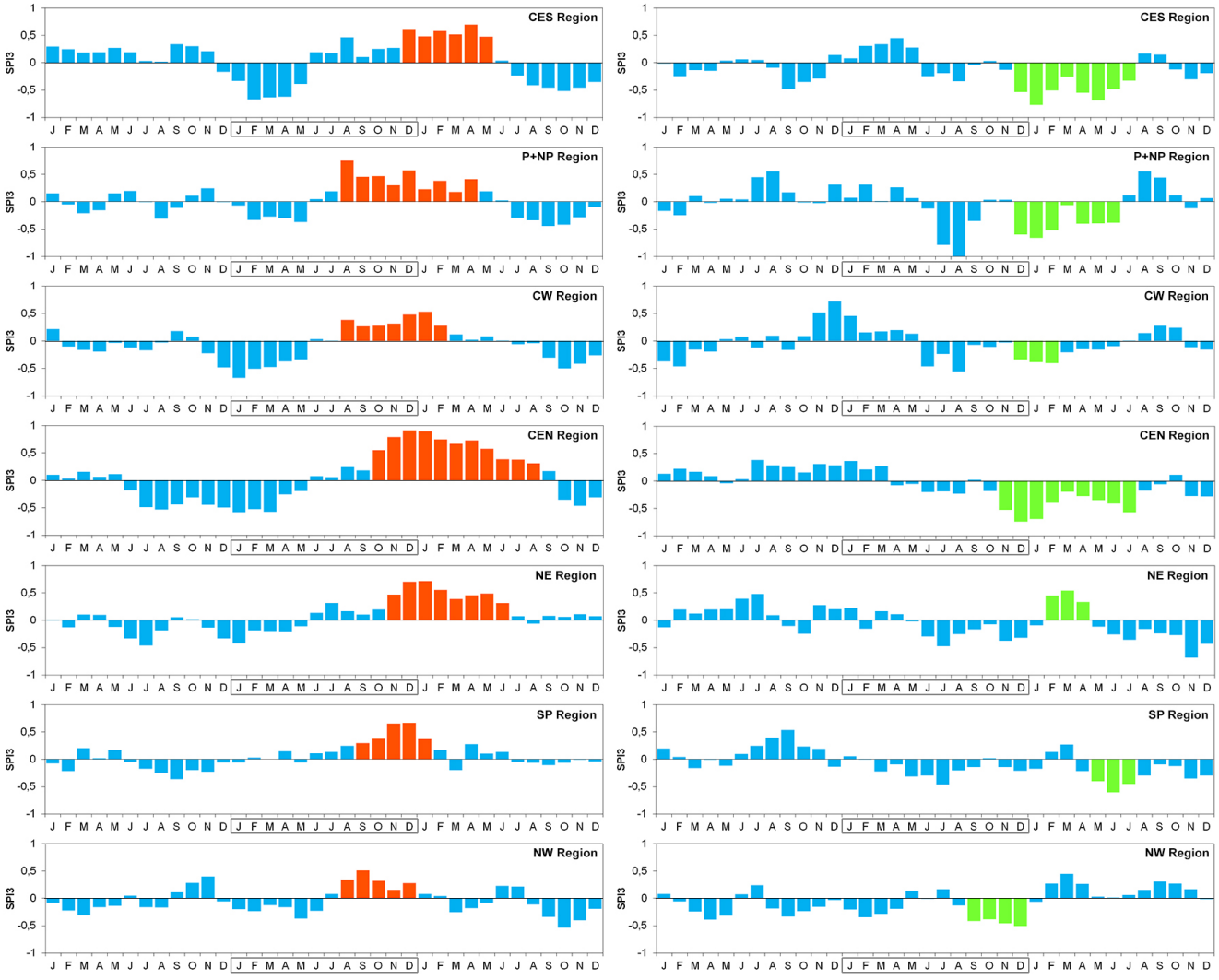

Figure 4. Regional aggregate SPI3 composites during El Niño (left) and La Niña (right) events. The months in the box refer to El Niño or La Niña years (0). Red (green) bars highlight the months of possible El Niño (La Niña) influence on the SPI3 time series.

cipitation is opposite to the one observed in the case of El Niño, with negative anomalies in precipitation. However, the response is not often clear in time and is detailed below. The CES region shows a signal associated with La Niña events between the months of December (0) to July (+), which is two months larger than in the case of El Niño signal. In the case of the P + NP region, the SPI3 significant anomalies are observed between December (0) and June (+), with negative SPI3 anomalies. Even when there is another period of significant negative anomalies, between the months of July (0) and September (0), it is considered that the signal is not consistent over time since the anomalies during October (0) and November (0) are positive. The months of August (+) and September (+) have significant positive SPI3 anomalies, which indicates that there is a strong seasonality associated to La Niña occurrences over the P + NP region. The influence of La Niña events in the precipitation of the CW region is observed in the austral summer after the La Niña development, although there are significant negative anomalies in the winter of the year 0. In the CEN region, the negative anomalies between November (0) to July (+) can be identified as La Niña influence. The NE region is characterized by both positive and negative significant anomalies associated to La Niña, indicating a strong seasonality in the SPI3 composites. This pattern is also a result of different impacts associated to La Niña years, with some years with above average precipitation and others with deficit conditions. The most consistent response is observed during the months of February–March–April (+), with positive SPI3 anomalies. The months of July, November and December of both the years 0 and + shows negative significant anomalies but do not form a consistent response over time. Moreover, most of the months between autumn (0) to the year following La Niña onset shows negative SPI3 composites, in line with the general regional be-

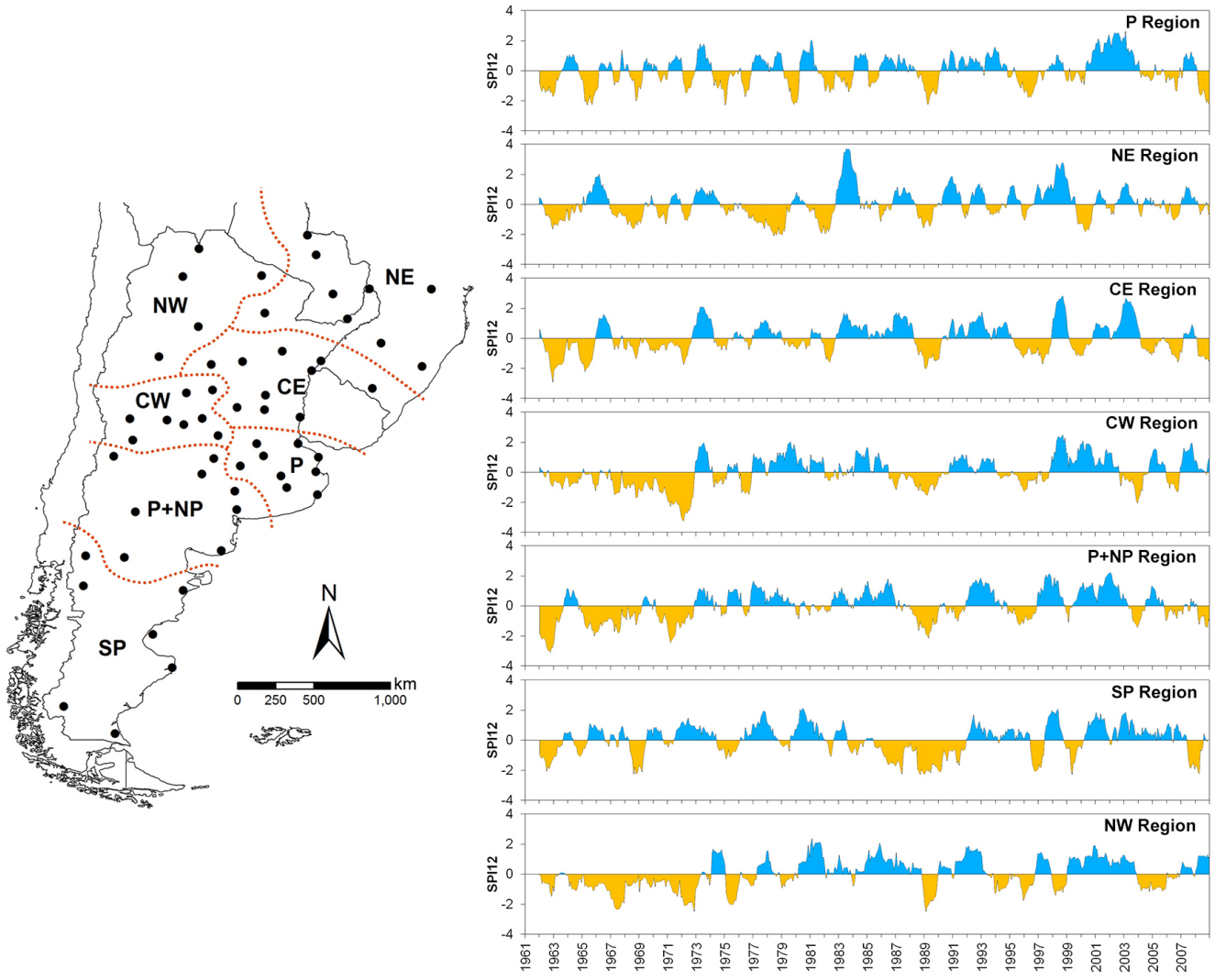

Figure 5. Same as Fig. 3 for the SPI12 time series.

havior and highlighting the heterogeneous precipitation response during La Niña events. The SP is characterized by a signal in precipitation during the months of May–June–July (+), while in the NW region this is observed in the months of September (0) to December (0). In the NW region significant positive and negative anomalies are observed in March (+) and September (+). The most relevant influence, both in time and intensity, of La Niña events in the regional precipitation for the time scale of 3 months is observed in the CES and CEN regions.

4.2 El Niño and La Niña signal in precipitation over SSA: SPI12

In the case of the regionalization of the SPI12 time series, seven homogeneous precipitation patterns were obtained (Fig. 5). The regions NW, NE, CW, P + NP and SP possess a similar spatial extent regarding the regionalization obtained for the SPI3. The Central-East (CE) and Pampas (P) appear as a combination of the regions CEN and CES, and CES and P + NP, respectively. Figure 5 shows the regional SPI12 time series, ordered by the explained variance from the RPCA. Given the reduction of the high frequency variability in comparison with the SPI3 temporal variations, regional dry and wet periods can be identified in a better way. Dry periods stand out during the 1960s and 1970s in several of the regions, which affected with drought conditions up to 60 % of the locations over the study area (Rivera and Penalba, 2014). Comparing these regional patterns with the ones obtained for the SPI3, it is observed that SPI responds more slowly to changes in precipitation, with less frequent but longer dry and wet periods.

Figure 6 shows the 36-month composites of the SPI12 during El Niño (left panel) and La Niña (right panel) years and its significant signal. It is noted that, even when the region-

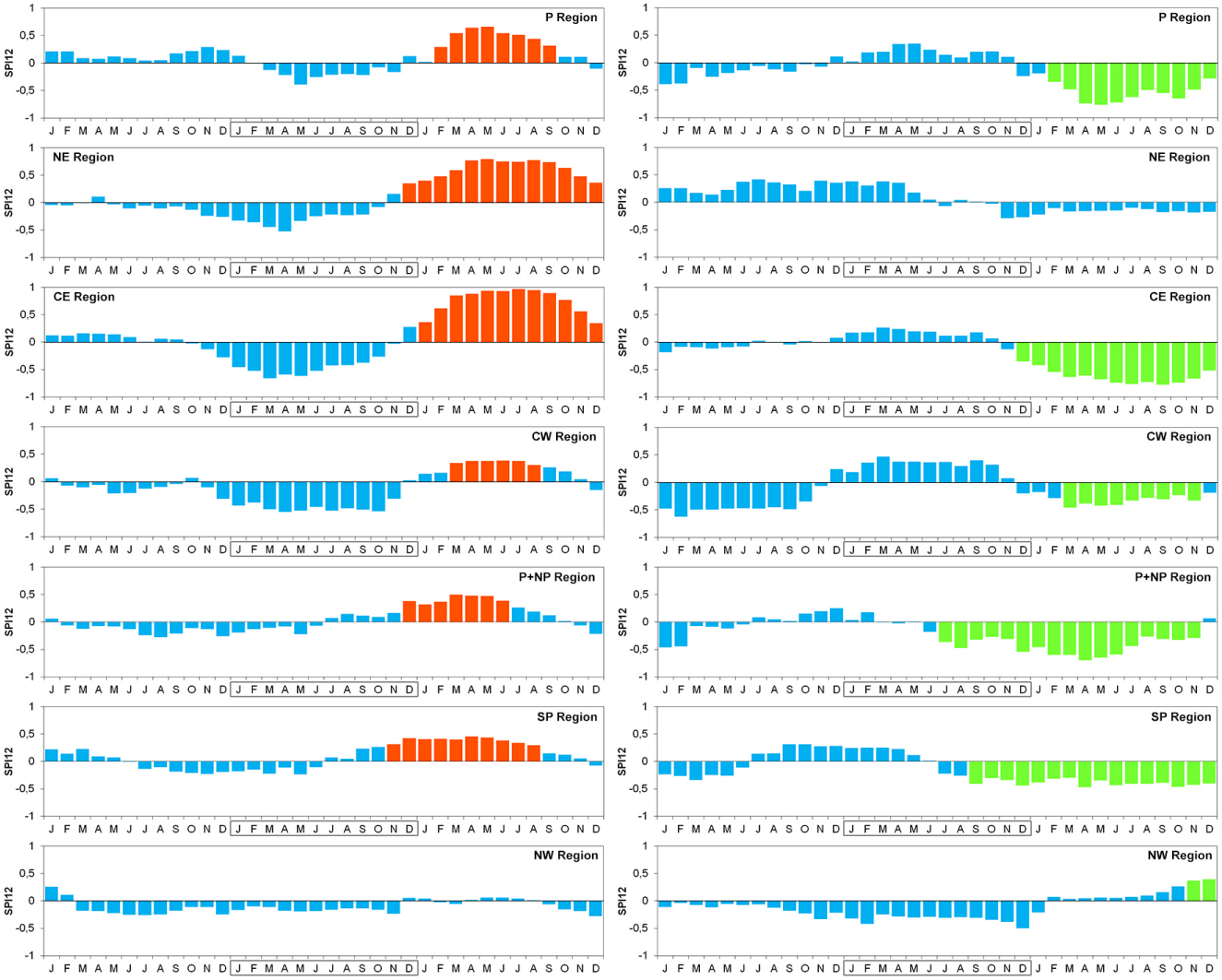

Figure 6. Same as Fig. 4 for SPI12.

alization is different from the obtained for the SPI3 time series and a direct comparison is not feasible, the response is more consistent in time and space, with a well-defined signal in most of the regions, associated to the filtering of the high-frequency variations of precipitation. Also, due to the increase in the time scale in which the accumulated precipitation is considered, the response is delayed in time with respect to the results observed for SPI3. In coherence with the findings for the SPI3 regional assessment, the sign of the anomalies of precipitation in the case of El Niño events is positive, while is negative in the case of La Niña events. The composite of SPI12 values during El Niño events over the P region presents a significant response between February (+) to September (+). The NE region has the longest temporal El Niño signal, from December (0) to December (+). Significant anomalies in the CE region occur during all the year following the development of El Niño and the intensity is higher compared to other regions, with SPI12 composite values close to 1. The wet period from March (+) to August (+) in the CW region is associated with El Niño signal, although it has small amplitude. In the P + NP region the signal is observed between December (0) to June (+), while the SP shows significant precipitation anomalies during November (0) to August (+). There is no evidence of El Niño influence on SPI12 time series in the NW region, which indicates that the accumulation of precipitation on time scales longer than 3 months creates a mixture of processes that influence regional precipitation patterns generating a poor signal associated with El Niño. It is remarkable the occurrence of consistent negative SPI12 composite values during the development of El Niño events, mainly in NE, CE and CW regions.

In the case of precipitation response to La Niña events (Fig. 6, right panel), the signal in P region is significant between February (+) and December (+), being 3 months

longer than El Niño signal. The difference between the precipitation response to El Niño and La Niña events is noteworthy in the NE region, where during La Niña conditions only November (0) shows a significant signal. Taking into account that the region has a spatial extension similar to the results from the SPI3 regionalization (Fig. 3), this poor signal can be attributed to different precipitation patterns recorded during La Niña years, which led to an inconsistent response over the region. In the CE region, the response is similar to the one observed during El Niño events, but opposite in sign, extending through all the year +. Precipitation over the CW region shows a coherent signal from March (+) to November (+), although the anomalies in August (+) and October (+) are not significant. The precipitation response to La Niña in P + NP region is noticeable extended over time with respect to the El Niño years, from July (0) to November (+). SP region shows a La Niña signal in precipitation patterns during the whole year + and the spring of the year 0, but with moderate values of the SPI12 composites. Finally, it is observed that the response in the NW region is restricted to the months of November (+) and December (+), with positive SPI12 composites during most of the year +. When the signal of El Niño and La Niña are compared, it is evident that there is a signal in precipitation that is more extended in time during La Niña years. This could be linked to the occurrences of La Niña events extending beyond one year, which can extend the precipitation response.

4.3 SST composites during regional drought conditions

Based on the results of the previous sections, it was observed that the influence of La Niña events resulted in the occurrence of precipitation deficits with different regional responses, both in duration and magnitude for time. This is associated to a teleconnection pattern that leads to negative moisture anomalies and subsidence over much of SSA (Grimm and Ambrizzi, 2009). These conditions favored the development of drought conditions, as reported by Grimm et al. (2000); Minetti et al. (2007); Chen et al. (2010) and Rivera and Penalba (2014), among others. In order to identify the influence of La Niña in the development of regional drought conditions over SSA, we analyzed the SST composites over the surrounding oceans during the months with SPI values below −1.0, a threshold usually chosen to define droughts (Lloyd-Hughes and Saunders, 2002). Similar assessments were carried out by Phillips and Denning (2007) for the analysis of extreme daily precipitation and its relationship with synoptic weather conditions and by Sienz et al. (2007), who analyzed the relationship between extreme SPI values and its relationship with mid-level circulation patterns, among others.

Figure 7 shows the composites of the SST anomalies for the months with drought conditions during the period 1961–2008 based on the regional SPI3 time series. Analogous results can be obtained for the SST composites based on the months with SPI12 values below −1.0, with an increase in the magnitude of the anomalies, considering a lag of approximately 7 months (not shown). This is in line with the lag observed between the La Niña peak (Fig. 2) and the maximum in the SPI12 signal during the following year (Fig. 6). The configuration of SST anomalies associated with drought events shows a clear La Niña pattern for most of the regions, with negative SST anomalies along the tropical Pacific. This stands out for the CES, P + NP, CW, CEN and NE regions. The NE region shows a clear link between drought occurrences and cold SST anomalies, a result that was not obvious considering the SPI3 composites from Fig. 4.

The spatial pattern of SST anomalies during drought conditions for the CES region has its greatest negative anomalies in the Niño 3 and Niño 1 + 2 region, while the pattern of the CW region has its major anomalies just in the Niño 3 region (Fig. 7). SST anomalies related to droughts over CEN region are located mainly over Niño 3.4 region, while in the case of the NE region the higher SST anomalies in the Niño 3 and Niño 1 + 2 regions. Droughts over SP also show a similar spatial pattern, although the magnitude of the anomalies is lower, located mainly in the Niño 1 + 2 region (Fig. 7). The spatial pattern of SST anomalies during droughts events over the NW region shows small areas with significant values, indicating a weak relationship to La Niña conditions. This is consistent with the results from the previous sections regarding the regional precipitation response for both SPI3 and SPI12 regional time series. Another interesting feature is the presence of negative SST anomalies along the coast of Brazil related to regional drought occurrences over CES and CEN regions. Due to the proximity of the SST anomalies to the above mentioned regions, localized cooling conditions leading to subsidence and lack of precipitation can influence the regional drought occurrences. This region of cold anomalies is not evident in the composites based on SPI12 time series (not shown), indicating that some areas of the South Atlantic Ocean modulate the seasonal precipitation patterns over SSA, as previously shown by Berri and Bertossa (2004) and Taschetto and Wainer (2008).

If we consider the composites for the months in which more than 30 % of the meteorological stations over SSA show drought conditions – defined as critical dry months (Krepper and Zucarelli, 2012; Penalba and Rivera, 2016), we obtain for the SPI3 a SST anomalies pattern similar to the one related to the CEN region and for the SPI12 a spatial pattern that resembles the results for the P + NP region (result not shown). This verifies that La Niña events can trigger drought conditions simultaneously over several regions, as is shown in Vicente-Serrano et al. (2011) for different time scales. The analysis can be extended to different drought categories, which are defined for different SPI thresholds, for instance, moderate ($-1.5 < \mathrm{SPI} \leq -1.0$), severe ($-2.0 < \mathrm{SPI} \leq -1.5$) and extreme ($\mathrm{SPI} \leq -2.0$) drought conditions. Nevertheless, it should be noted

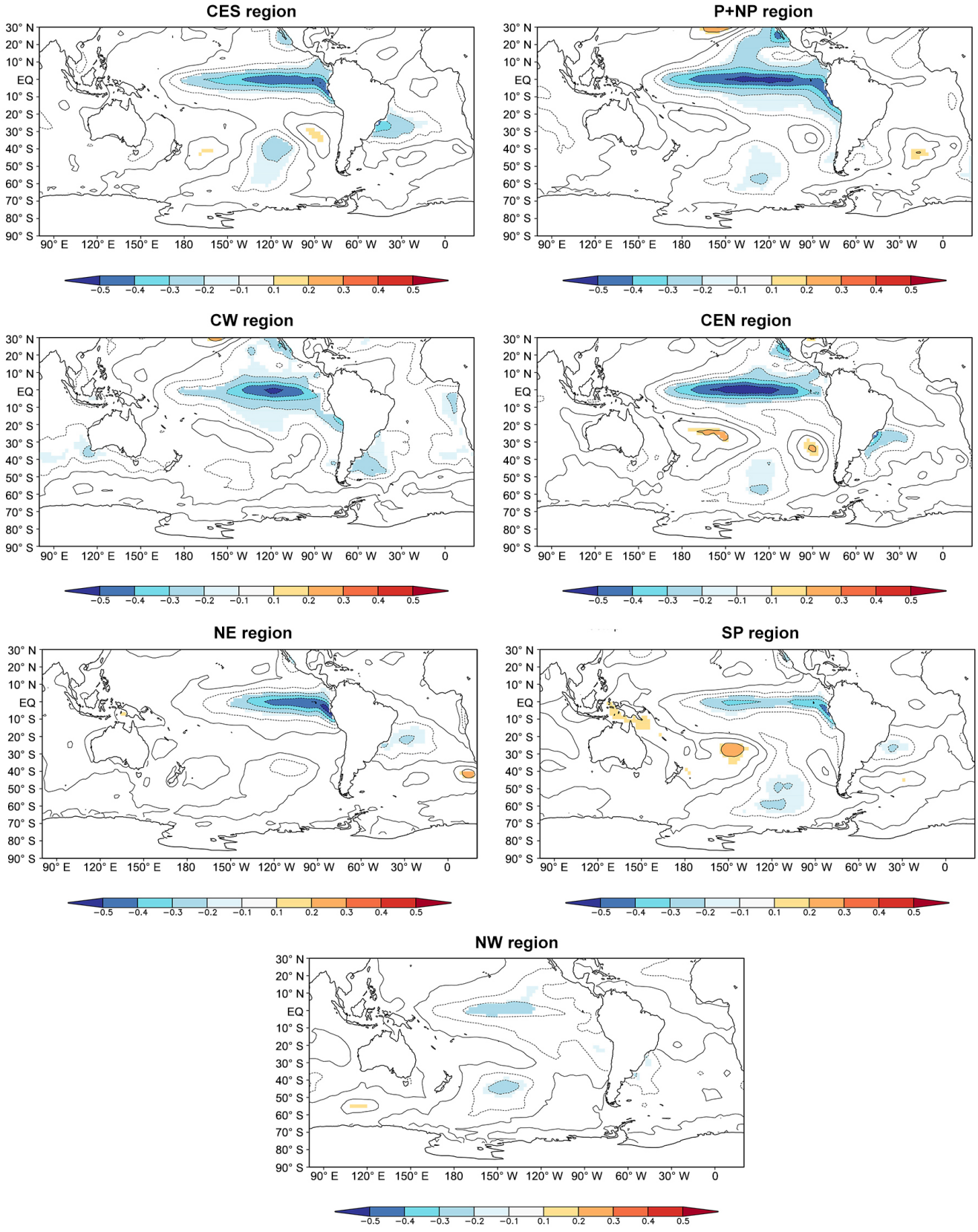

Figure 7. Composites of SST anomalies during the months with drought conditions for each of the seven regional SPI3 patterns. Shaded areas are significant at the 95 % level.

that the sample size can be reduced considerably, leading to limitations in the results.

5 Discussion and conclusions

The ENSO phenomenon has a strong impact on precipitation in SSA, both at seasonal to interannual time scales, associated to its two phases: El Niño and La Niña. Links between precipitation patterns and ENSO signal were assessed extensively both at regional and global scales, in order to improve the monitoring and forecasting of its impacts. However, some gaps remain regarding the ENSO prediction and its expected remote impacts, as stated in Kirtman et al. (2013). In order to advance in the knowledge between El Niño and La Niña occurrences and the regional patterns of precipitation, this research analyzed the precipitation response to the ENSO phases taking into account the regional features of precipitation over SSA. In order to quantify precipitation departures, we selected the SPI, given that it allows the comparison of time series from regions with different climate conditions. Other studies using for example the PDSI faced problems to compare individual time series (Piechota and Dracup, 1996), one of the many limitations of the index (Hayes et al., 1999). Percentiles based on an appropriate probability distribution were commonly used to identify El Niño/La Niña signal on hydroclimatological records (Dracup and Kahya, 1994; Karabork and Kahya, 2003). Nevertheless, the SPI is widely considered the most robust and effective index (Vicente-Serrano et al., 2005), proved to be a good indicator of both wet (Seiler et al., 2002) and dry (Penalba and Rivera, 2015) events, and it can be calculated at different time scales, allowing the monitoring of different drought types. The magnitude of departure from zero represents a probability of occurrence so that decisions can be made based on this SPI value (Hayes et al., 1999). When the time scale is short, for instance 3-month, the SPI reflect the seasonality of the data and is more appropriate to identify drought impacts on agriculture (Moreira et al., 2008). For time scale of 12 months, the SPI can reflect changes that are relevant for hydrological drought analyses and applications. Therefore, it is relevant to analyze the signal of El Niño/La Niña events in precipitation at different time scales, in order to discuss possible differences and the applicability of the findings.

In order to identify the regional features of precipitation, RPCA were applied to the 56 SPI time series at time scales of 3 and 12 months. This approach differs to the typical assessment based on harmonical fit to the precipitation composites and vectorial coherence, following the works of Ropelewski and Halpert (1986, 1987). The regionalization allowed to obtain seven homogeneous regions for both time scales, which are climatically and geographically consistent, that can be useful to obtain not only the El Niño and La Niña signals, but also other forcings related to precipitation over SSA. Through a bootstrap resampling procedure, significant SPI composites were identified for both El Niño and La Niña, with a reversal in sign of the SPI composites during the El Niño phase (wet conditions) compared to those during La Niña phase (dry conditions). The consistency of the signal shows differences between the two phases, being more consistent during El Niño events and less consistent during La Niña, particularly for SPI3. The length and intensity of the signal is regionally dependent. In the case of the SPI3, the most relevant signal associated to El Niño occurrences was obtained for the precipitation time series of the CEN, CES, P + NP and NE regions (Fig. 4), ranging from 6 to 11 months. The SPI3 response to La Niña events shows that the most relevant influence, both in time and intensity, was observed in the CES and CEN regions. However, there is a clear seasonality in the SPI3 composites, mainly over the CES, CEN and P + NP regions, which can lead to agricultural impacts if different flavors of La Niña are not assessed. This is also evident in the response associated to the SPI12 over the NE region (Fig. 6), and in other regions and variables, like the snowpack variations and the streamflow records over the Central Andes (Masiokas et al., 2006). The SPI12 response to La Niña events has an average duration of approximately one year, being longer than for El Niño events. This could be linked to the occurrences of La Niña events that last longer than one year, which can extend the precipitation response. Mechanisms related to this kind of sustained La Niña events still not fully understood (Kirtman et al., 2013); therefore, advances in this topic can be helpful to understand the different impacts on regional precipitation, especially for drought conditions.

It is difficult to make a contrast between the results obtained in this research and those reported in the literature for the study region, given the different methodologies applied, the different periods considered and the time scales used for the accumulation of precipitation. However, the consistency in the sign of the SPI composites during El Niño/La Niña events is in agreement with the results obtained by previous research.

The analysis of SST composite anomalies during regional drought conditions shows a clear La Niña pattern for most of the regions, with a cold tongue extending over the Tropical Pacific (Fig. 7). Even when the most used El Niño definition is based on the El Niño 3.4 region (Trenberth, 1997), the area of strong SST anomalies associated to drought conditions has some regional variations. For example, for some of the precipitation regions a better response can be obtained analyzing the SST anomalies in the El Niño 1 + 2 area, like for the NE region. This indicate that the precipitation response can be dependent upon the box in which the El Niño index is constructed. Moreover, a separation between typical El Niño pattern and El Niño Modoki (Ashok et al., 2007) can also be helpful in understanding the differences in the precipitation responses. In the case of the SST composites associated with months with drought over the CEN and CES regions, it is evident a contribution of the South Atlantic Ocean in the mod-

ulation of seasonal SPI3, with cooling conditions that can lead to subsidence and below average precipitation. Further research is needed to determine if this local cooling responds to remote Tropical Pacific conditions or if it is a different source of seasonal variability. In this sense, to consider only the ENSO as the solely responsible for the precipitation temporal variability over the SSA prevents the development of a successful prediction tool, hence, other modes of variability should be considered on several time scales.

Acknowledgements. We thank S. M. Vicente-Serrano and one anonymous referee for their valuable comments and critical reading of the manuscript. The research leading to these results received funding from the European Community's Seventh Framework Programme (FP7/2007–2013: CLARIS LPB. A Europe–South America Network for Climate Change Assessment and Impact Studies in La Plata Basin), by the University of Buenos Aires (Grant UBA-20020130200142BA) and the Argentinean Council of Scientific and Technical Research (Grant PIP 0227).

Edited by: J. D. Pabón-Caicedo
Reviewed by: S. M. Vicente Serrano and one anonymous referee

References

Aceituno, P.: On the functioning of the Southern Oscillation in the South American sector – Part I: Surface climate, Mon. Weather Rev., 116, 505–524, 1988.

Alexandersson, H.: A homogeneity test applied to precipitation data, J. Climatol., 6, 661–675, 1986.

Anderson, T. W. and Darling, D. A.: Asymptotic theory of certain "Goodness of Fit" criteria based on stochastic processes, Ann. Math. Stat., 23, 193–212, 1952.

Antico, A., Torres, M. E., and Diaz, H. F.: Contributions of different time scales to extreme Paraná floods, Clim. Dynam., doi:10.1007/s00382-015-2804-x, online first, 2015.

Ashok, K., Behera, S. K., Rao, S. A., Weng, H., and Yamagata, T.: El Niño Modoki and its possible teleconnection, J. Geophys. Res., 112, C11007, doi:10.1029/2006JC003798, 2007.

Barros, V. R., Doyle, M. E., and Camilloni, I. A.: Precipitation trends in southeastern South America: relationship with ENSO phases and with low-level circulation, Theor. Appl. Climatol., 93, 19–33, 2008.

Berri, G. J. and Bertossa, G. I.: The influence of the Tropical and Subtropical Atlantic and Pacific oceans on precipitation variability over Southern Central South America on seasonal time scales, Int. J. Climatol., 24, 415–435, 2004.

Boulanger, J.-P., Leloup, J., Penalba, O., Rusticucci, M., Lafon, F., and Vargas, W.: Low-frequency modes of observed precipitation variability over the La Plata Basin, Clim. Dynam., 24, 393–413, 2005.

Camilloni, I. and Barros, V.: Extreme discharge events in the Paraná River and their climate forcing, J. Hydrology, 278, 94–106, 2003.

Cattell, R. B.: The screen test for the number of factors, J. Multiv. Behav. Res., 1, 245–276, 1966.

Chamorro, L.: Los principales usos y problemas de los recursos hídricos, in: El Cambio climático en la cuenca del Plata, Buenos Aires, edited by: Barros, V., Clarke, R., and Silva Dias, P., CIMA/CONICET, 111–123, 2006.

Chen, J. L., Wilson, C. R., Tapley, B. D., Longuevergne, L., Yang, Z. L., and Scanlon, B. R.: Recent La Plata basin drought conditions observed by satellite gravimetry, J. Geophys. Res., 115, D22108, doi:10.1029/2010JD014689, 2010.

Chiew, F. H. S., Piechota, T. C., Dracup, J. A., and McMahon, T. A.: El Niño/Southern Oscillation and Australian rainfall, streamflow and drought: Links and potential for forecasting, J. Hydrology, 204, 138–149, 1998.

Compagnucci, R. H. and Vargas, W. M.: Interannual variability of Cuyo rivers streamflow in Argentinean Andean Mountains and ENSO events, Int. J. Climatol., 18, 1593–1609, 1998.

Comrie, A. C. and Glenn, E. C.: Principal components-based regionalization of precipitation regimes across the southwest United States and northern Mexico, with an application to monsoon precipitation variability, Clim. Res., 10, 201–215, 1998.

Dracup, J. A. and Kahya, E.: The relationships between U.S. streamflow and La Niña events, Water Resour. Res., 30, 2133–2141, 1994.

Edwards, D. C. and McKee, T. B.: Characteristics of 20th century drought in the United States at multiple time scales, Atmospheric Science Paper No. 634, Climatology Report No. 97-2, Department of Atmospheric Sciences, Colorado State University, Fort Collins, CO, 1997.

Efron, B. and Tibshirani, R. J.: An Introduction to the Bootstrap, Chapman & Hall, International Thomson Publication, New York, USA, 1993.

González, M. H. and Vera, C. S.: On the interannual winter rainfall variability in Southern Andes, Int. J. Climatol., 30, 643–657, 2010.

Grimm, A. M. and Ambrizzi, T.: Teleconnections into South America from the Tropics and Extratropics on Interannual to Intraseasonal Timescales, in: Past Climate Variability in South America and Surrounding Regions, edited by: Vimeux, F., Dev. Paleoenviron. Res., 14, 159–191, doi:10.1007/978-90-2672-9_7, Springer, 2009.

Grimm, A. M., Barros, V. R., and Doyle, M. E.: Climate variability in Southern South America associated with El Niño and La Niña events, J. Climate, 13, 35–58, 2000.

Guttman, N. B.: Accepting the standardized precipitation index: A calculation algorithm, J. Am. Water Resour. As., 35, 311–322, 1999.

Hayes, M. J., Svoboda, M. D., Wilhite, D. A., and Vanyarkho, O. V.: Monitoring the 1996 drought using the standardized precipitation index, B. Am. Meteorol. Soc., 80, 429–438, 1999.

Hayes, M., Svoboda, M., Wall, N., and Widhalm, M.: The Lincoln Declaration on Drought Indices: Universal meteorological drought index recommended, B. Am. Meteorol. Soc., 92, 485–488, 2011.

Hisdal, H. and Tallaksen, L. M.: Estimation of regional meteorological and hydrological drought characteristics: a case study for Denmark, J. Hydrol., 281, 230–247, 2003.

Kaiser, H. F.: The Varimax criterion for analytic rotation in factor analysis, Psychometrika, 23, 187–200, 1958.

Karabork, M. C. and Kahya, E.: The teleconnections between the extreme phases of the Southern Oscillation and precipitation patterns over Turkey, Int. J. Climatol., 23, 1607–1625, 2003.

Kirtman, B., Anderson, D., Brunet, G., Kang, I.-S., Scaife, A. A., and Smith, D.: Prediction from Weeks to Decades, in: Climate Science for Serving Society – Research, Modeling and Prediction Priorities, edited by: Asrar, G. R. and Hurrell, J. W., 205–235, Springer, New York, USA, 2013.

Krepper, C. M. and Zucarelli, V.: Climatology of Water Excess and Shortages in the La Plata Basin, Theor. Appl. Climatol., 102, 13–27, 2012.

Lloyd-Hughes, B. and Saunders, M. A.: A drought climatology for Europe, Int. J. Climatol., 22, 1571–1592, 2002.

Masiokas, M., Villalba, R., Luckman, B., Le Quesne, C., and Aravena, J. C.: Snowpack variations in the Central Andes of Argentina and Chile, 1951–2005: Large-scale atmospheric influences and implications for water resources in the region, J. Climate, 19, 6334–6352, 2006.

McKee, T. B., Doesken, N. J., and Kleist, J.: The relationship of drought frequency and duration to time scales, in: Proceedings of the Eight Conference on Applied Climatology, Anaheim, CA, American Meteorological Society, 179–184, 1993.

Minetti, J. L., Vargas, W. M., Poblete, A. G., Acuña, L. R., and Casagrande, G.: Non-linear trends and low frequency oscillations in annual precipitation over Argentina and Chile, 1931–1999, Atmósfera, 16, 119–135, 2003.

Moreira, E. E., Coelho, C. A., Paulo, A. A., Pereira, L. S., and Mexia, J. T.: SPI-based drought category prediction using loglinear models, J. Hydrol., 354, 116–130, 2008.

Mudelsee, M.: The Bootstrap in Climate Risk Analysis, in: Extremis – Disruptive Events and Trends in Climate and Hydrology, edited by: Kropp, J. and Schellnhuber, H.-J., 44–58, ISBN: 978-3-642-14863-7, 2011.

Paruelo, J. M., Beltrán, A., Jobbágy, E., Sala, O. E., and Golluscio, R. A.: The climate of Patagonia: general patterns and controls on biotic processes, Ecología Austral., 8, 85–101, 1998.

Pasquini, A. I., Lecomte, K. L., Piovano, E. L., and Depetris, P. J.: Recent rainfall and runoff variability in central Argentina, Quat. Int., 158, 127–139, 2006.

Penalba, O. C. and Rivera, J. A.: Uso de la distribución de probabilidades gamma para la representación de la precipitación mensual en el Sudeste de Sudamérica, Cambios espacio-temporales en sus parámetros, in: Proceedings of the XI CONGREMET, Mendoza, Argentina, 28 May–1 June, 2012.

Penalba, O. C. and Rivera, J. A.: Comparación de seis índices para el monitoreo de sequías meteorológicas en el sur de Sudamérica, Meteorológica, 40, 33–57, 2015.

Penalba, O. C. and Rivera, J. A.: Regional aspects of future precipitation and meteorological drought characteristics over Southern South America projected by a CMIP5 multi-model ensemble, Int. J. Climatol., 36, 974–986, 2016.

Penalba, O. C., Beltran, A., and Messina, C.: Monthly rainfall in central-eastern Argentina and ENSO: a comparative study of rainfall forecast methodologies, Rev. Bras. Agrometeorologia, 13, 49–61, 2005.

Penalba, O. C., Pántano, V. C., Spescha, L. B., and Murphy, G. M.: ENSO impact on dry sequences during different phenological periods in the east-northeast of Argentina, III International Conference on ENSO: Bridging the gaps between global ENSO science and regional processes, extremes and impacts, Guayaquil, Ecuador, 12–14 November, 2014a.

Penalba, O. C., Rivera, J. A., and Pántano, V. C.: The CLARIS LPB database: constructing a long-term daily hydro-meteorological dataset for La Plata Basin, Southern South America, Geosci. Data J., 1, 20–29, 2014b.

Penalba O. C., Rivera J. A., Pántano, V. C., and Bettolli, M. L.: Extreme rainfall and hydric condition in Southern La Plata Basin and the associated atmospheric circulation, Clim. Res., doi:10.3354/cr01353, online first, 2016.

Penland, C., Sun, D.-Z., Capotondi, A., and Vimont, D. J.: A brief introduction of El Niño and La Niña, in: Climate dynamics: Why does climate vary?, edited by: Sun, D.-Z. and Bryan, F., Geophys. Monogr. Ser., 189, 53–64, American Geophysical Union, Washington, USA, 2010.

Piechota, T. C. and Dracup, J. A.: Drought and regional hydrologic variation in the United States: Associations with the El Niño-Southern Oscillation, Water Resour. Res., 32, 1359–1373, 1996.

Phillips, I. D. and Denning, H.: Winter daily precipitation variability over the South West Peninsula of England, Theor. Appl. Climatol., 87, 103–122, 2007.

Podestá, G. P., Messina, C. D., Grondona, M. O., and Magrin, G. O.: Associations between grain crop yields in central-eastern Argentina and El Niño-Southern Oscillation, J. Appl. Meteorol., 38, 1488–1498, 1999.

Prieto, M. R., Herrera, R., and Dussel, P.: Historical Evidences of the Mendoza River Streamflow Fluctuations and their Relationship with ENSO, Holocene, 9, 473–471, 1999.

Richman, M.: Rotation of Principal Components, J. Climatol., 6, 293–335, 1986.

Rivera, J. A. and Penalba, O. C.: Trends and spatial patterns of drought affected area in Southern South America, Climate, 2, 264–278, 2014.

Rivera, J. A., Araneo, D. C., and Penalba, O. C.: Evaluación del período de crisis hídrica 2010–2014 en la región de Cuyo, XII Congreso Argentino de Meteorología, Mar del Plata, Argentina, 26–29 May, 2015.

Ropelewski, C. F. and Halpert, M. S.: North American precipitation and temperature patterns associated with the El Niño/Southern Oscillation (ENSO), Mon. Weather Rev., 114, 2352–2362, 1986.

Ropelewski, C. F. and Halpert, M. S.: Global and regional scale precipitation patterns associated with the El Niño/Southern Oscillation, Mon. Weather Rev., 115, 1606–1626, 1987.

Russián, G. F., Agosta, E. A., and Compagnucci, R. H.: Variabilidad interanual a interdecádica de la precipitación en Patagonia Norte, Geoacta, 35, 27–43, 2010.

Schonher, T. and Nicholson, S. E.: The relationship between California rainfall and ENSO events, J. Climate, 2, 1258–1269, 1989.

Seiler, R. A., Hayes, M., and Bressan, L.: Using the standardized precipitation index for flood risk monitoring, Int. J. Climatol., 22, 1365–1376, 2002.

Sienz, F., Bordi, I., Fraedrich, K., and Schneidereit, A.: Extreme dry and wet events in Iceland: observations, simulations and scenarios, Meteorol. Z., 16, 9–16, 2007.

Silvestri, G. E. and Vera, C. S.: Antarctic Oscillation signal on precipitation anomalies over southeastern South America, Geophys. Res. Lett., 30, 2115, doi:10.1029/2003GL018277, 2003.

Smith, T. M., Reynolds, R. W., Peterson, T. C., and Lawrimore, J.: Improvements to NOAA's Historical Merged Land-Ocean Surface Temperature Analysis (1880–2006), J. Climate, 21, 2283–2296, 2008.

Spescha, L., Forte Lay, J., Scarpati, O., and Hurtado, R.: Los excesos de agua edáfica y su relación con el ENSO en la región Pampeana, Rev. Facultad de Agronomía, 24, 161–167, 2004.

Taschetto, A. S. and Wainer, I.: The impact of the subtropical South Atlantic SST on South American precipitation, Ann. Geophys., 26, 3457–3476, doi:10.5194/angeo-26-3457-2008, 2008.

Trenberth, K. E.: Signal versus Noise in the Southern Oscillation, Mon. Weather Rev., 112, 326–332, 1984.

Trenberth, K. E.: The definition of El Niño, B. Am. Meteorol. Soc., 78, 2771–2777, 1997.

Trenberth, K. E. and Stepaniak, D. P.: Indices of El Niño evolution, J. Climate, 14, 1697–1701, 2001.

Vicente-Serrano, S. M.: El Niño and La Niña influence on droughts at different timescales in the Iberian Peninsula, Water Resour. Res., 41, W12415, doi:10.1029/2004WR003908, 2005.

Vicente-Serrano, S. M., López-Moreno, J. I., Gimeno, L., Nieto, R., Morán-Tejada, E., Lorenzo-Lacruz, J., Beguería, S., and Azorin-Molina, C.: A multiscalar global evaluation of the impact of ENSO on droughts, J. Geophys. Res., 116, D20109, doi:10.1029/2011JD016039, 2011.

Wolter, K. and Timlin, M. S.: Monitoring ENSO in COADS with a seasonally adjusted principal component index, Proceedings of the 17th Climate Diagnostics Workshop, Norman, Oklahoma, NOAA/NMC/CAC, NSSL, Oklahoma Clim. Survey, CIMMS and the School of Meteor., Univ. of Oklahoma, 52–57, 1993.